Journal of Biomolecular NMR, **19:** 103–113, 2001.
KLUWER/ESCOM

Pulse sequences for detection of $NH_2 \cdots N$ hydrogen bonds in sheared G·A mismatches via remote, non-exchangeable protons

Ananya Majumdar*, Abdelali Kettani, Eugene Skripkin & Dinshaw J. Patel
Cellular Biochemistry and Biophysics Program, Box 557, Memorial Sloan-Kettering Cancer Center, 1275 York Avenue, New York, NY 10021, U.S.A.

Received 1 September 2000; Accepted 22 November 2000

Key words: A·(G·G·G·G)·A hexad, G·A mismatch, G·(C–A) triad, G·G·G·G tetrad, H(C)NN(H), HNN–COSY, hydrogen bond, $^{2h}J_{NN}$, soft HNN–COSY

Abstract

The non-detectability of NH···N hydrogen bonds in nucleic acids due to exchange broadened imino/amino protons has recently been addressed via the use of non-exchangeable protons for detecting internucleotide $^{2h}J_{NN}$ couplings. In these applications, the appropriate non-exchangeable proton is separated by two bonds from the NH···N bond. In this paper, we extend the scope of this approach to protons which are separated by four bonds from the NH···N moiety. Specifically, we consider the case of the commonly occurring sheared G · A mismatch alignment, in which we use the adenine H2 proton to report on the (A)N6H6$_{1,2}$···N3(G) hydrogen bond, in the presence of undetectable, exchange broadened N6H6$_{1,2}$ protons. Two sequences, the 'straight-through' (H6)N6N3H2 and 'out–and–back' H2N6N3 experiments, are presented for observing these correlations in H_2O and D_2O solution, respectively. The sequences are demonstrated on two uniformly ^{15}N,^{13}C labelled DNA samples: d($G_1G_2G_3T_4T_5C_6A_7G_8G_9$)$_2$, containing a G3·(C6–A7) triad involving a sheared G3·A7 mismatch, and d($G_1G_2G_3C_4A_5G_6G_7T_8$)$_4$, containing an A5·(G3·G6·G3·G6)·A5 hexad involving a sheared G3·A5 mismatch.

Introduction

The detection of NH···N hydrogen bonds via $^{2h}J_{NN}$ correlated spectroscopy has become a cornerstone of nucleic acid structure determination by NMR (Dingley and Grzesiek, 1998; Pervushin et al., 1998; Majumdar et al., 1999a,b; Dingley et al., 1999, 2000; Wohnert et al., 1999; Jiang et al., 1999b; Kettani et al., 1999, 2000a,b; Dingley et al., 2000; Hennig and Williamson, 2000; Luy and Marino, 2000). Following the original HNN–COSY experiment (Dingley and Grzesiek, 1998; Pervushin et al., 1998), which correlates hydrogen bonded imino/amino protons with the donor and acceptor nitrogens, new methodology has evolved rapidly, such as the soft HNN–COSY (Majumdar et al., 1999a) and subsequent improvements (Dingley et al., 2000), for correlating far upfield donor nitrogens with far downfield acceptor nitrogens. The recent detection of $^{4h}J_{NN}$ (Liu et al., 2000) and $^{3h}J_{NCO}$ (Dingley et al., 2000) couplings to monitor N–H···C=O hydrogen bonds in nucleic acids, has further bolstered the possibilities in this field. These techniques have been applied not only to the identification of Watson-Crick base pairing (Dingley and Grzesiek, 1998; Pervushin et al., 1998; Dingley et al., 1999; Jiang et al., 1999b) but have also significantly impacted studies of higher order nucleic acid structures containing unusual motifs with non-canonical hydrogen bonding schemes. Applications to A·A (Kettani et al., 1999) and G·G mismatches (Kettani et al., 1999; Wohnert et al., 1999), tandem G·A mismatches (Wohnert et al., 1999), T·A and C^+·G Hoogsteen (Dingley et al., 1999) and A·U reverse Hoogsteen (Wohnert et al., 1999) base pairing, and sheared G·A mismatches (Kettani et al., 2000a, b) have been reported in a variety of contexts. As an important consequence, the identification of well-known struc-

*To whom correspondence should be addressed. E-mail: majumdar@sbnmr1.mskcc.org

tural elements such as G·G·G·G tetrads (Kettani et al., 2000a,b; Dingley et al., 2000) and G·C·G·C tetrads (Majumdar et al., 1999b) as well as novel motifs such as A·(G·G·G·G)·A hexads (Kettani et al., 2000a) and G·(C–A) triads (Kettani et al., 2000b) has been greatly facilitated through the use of $^{2h}J_{NN}$ correlated spectroscopy. One application of HNN–COSY to His–His side chain contacts in proteins (apomyoglobin) has also been reported (Hennig and Geierstanger, 1999). Reviews summarizing some of the above work have appeared recently (Gemmeker, 2000; Mollova and Pardi, 2000).

An important base pairing alignment observed in nucleic acids is the sheared G·A mismatch, in which the minor groove of guanine aligns with the major groove of adenine (Figure 1a). Sheared G·A mismatches have been observed as a frequent feature within structures of purine rich sequences in duplex DNA (Hirao et al., 1989, 1994; Li et al., 1991; Chou et al., 1992, 1997; Maskos et al., 1993), higher-order DNA architectures (Kettani et al., 2000a, b) and ligand–DNA aptamer complexes (Lin and Patel, 1997; Lin et al., 1998). They have also been detected as conserved building blocks in RNA architecture (Heus and Pardi, 1991; Szewczak et al., 1993; Jucker et al., 1996), in peptide–RNA complexes (Cai et al., 1998; Legault et al., 1998; Jiang et al., 1999a) and in ribozymes (Pley et al., 1994; Cate et al., 1996). The sheared G·A mismatch pair is characteristically involved in cross-strand stacking, and is unusual in that the Watson–Crick edges of both guanine and adenine are available for further base pair alignments.

From Figure 1a, it is seen that the sheared G·A mismatch is defined by two $NH_2 \cdots N$ hydrogen bonds involving (a) the guanine amino protons ($N2H2_{1,2}$) and N7 nitrogen of adenine and (b) the adenine amino protons ($N6H6_{1,2}$) and the N3 nitrogen of guanine. Under conditions of slow rotation of the NH_2 group about the exocyclic C2–N2 bond, the $(G)N2H2_{1,2} \cdots N7(A)$ bond may be identified using the soft HNN–COSY type of experiments (Majumdar et al., 1999a; Dingley et al., 2000), which correlate the guanine $N2H_2$ protons with the N7 nitrogens of adenine via the *trans*-hydrogen bond $^{2}J_{N2N7}$ coupling. Under similar circumstances, the $(A)N6H6_{1,2} \cdots N3(G)$ bond is easily addressed using the HNN–COSY experiment (Dingley and Grzesiek, 1998), to correlate the adenine $N6H_2$ protons with the guanine N3 nitrogen via the $^{2h}J_{N6N3}$ coupling.

A serious problem which plagues the detection of $^{2}J_{NN}$ couplings in nucleic acids is the vulnerability of both imino and amino protons to exchange broadening effects: imino protons are susceptible to chemical exchange with solvent, and amino protons are often rendered undetectable due to intermediate exchange resulting from rotation about the exocyclic C–N(H_2) bond. Under these conditions, the $(G)N2H_2 \cdots N7(A)$ may be identified using the H(CN)N(H) class of experiments (Majumdar et al., 1999b; Hennig and Williamson, 2000; Luy and Marino, 2000), in which the non-exchangeable H8 proton of adenine is correlated with the N2 nitrogen of guanine via the *trans*-hydrogen bond $^{2h}J_{N2N7}$ coupling. These experiments have been successfully applied to conclusively prove the existence of a G·C·G·C tetrad, a G·G·G·G tetrad and an A·(G·G·G·G)·A hexad in two separate DNA fragments (Majumdar et al., 1999b; Kettani et al., 2000a). Hennig and Williamson (2000) applied the same approach to the HIV TAR RNA–argininamide complex to unambiguously identify a previously debated U–A·U base triple, where the uridine imino proton involved in the reverse Hoogsteen A·U base pair was undetectable due to chemical exchange with water. Luy and Marino (2000) have carried out similar experiments to investigate NH···N bonds and their dynamics in RNA. In addition to solving the exchange broadening issue, the H(C)NN(H) type of experiments may also be carried out at higher temperatures, as well as in D_2O solution, and are therefore free of water-suppression and saturation transfer related problems.

The establishment of the $^{2h}J_{N6N3}$ coupling across the $(A)N6H_2 \cdots N3(G)$ hydrogen bond under exchange-broadened conditions, presents a far more difficult challenge, since the nearest non-exchangeable proton – H2 of adenine – is remotely located from the site of the hydrogen bond. In our laboratory, such a situation was encountered during an NMR study of the DNA quadruplex $d(G_1G_2G_3C_4A_5G_6G_7T_8)_4$, shown schematically in Figure 2a. NOE data suggested that the molecule adopts an A5·(G3·G6·G3·G6)·A5 hexad motif (detail shown in Figure 2b), similar to the A·(G·G·G·G)·A hexad observed previously in $d(GGAGGAG)_4$ (Kettani et al., 2000a). The hexad involves alignment of two structural motifs: a G3·G6·G3·G6 tetrad core and a sheared G3·A5 base pair, which is critical to the formation of the hexad. Evidence for the hexad came from $(G)NH_2 \cdots N7(A,G)$ cross peaks in soft HNN–COSY spectra (Majumdar et al., 1999a) and (A,G)H8···N2(G) cross peaks in H(C)NN(H) spectra (Majumdar et al., 1999b). However, a vi-

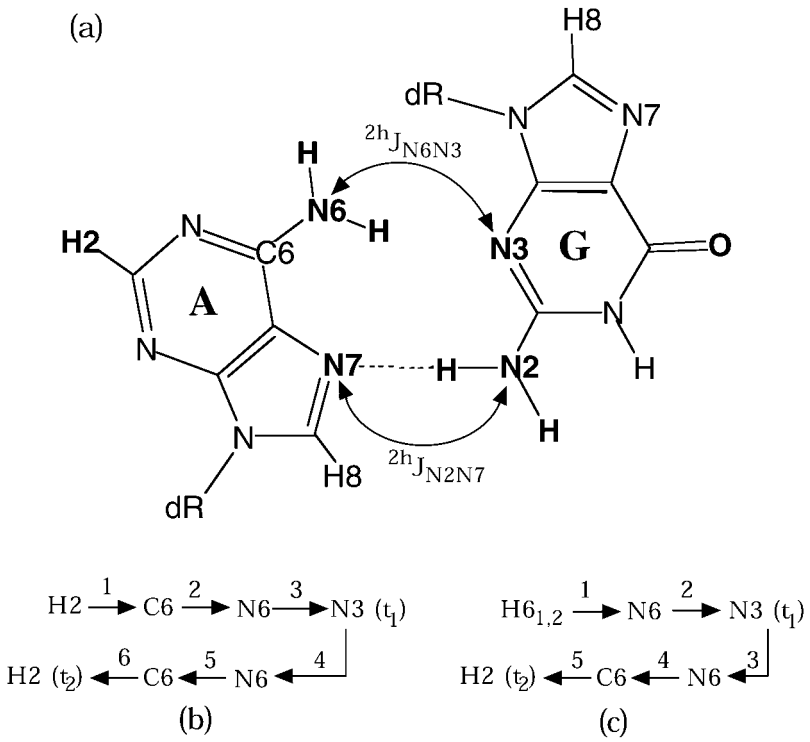

Figure 1. (a) Schematic of a sheared G·A mismatch indicating the (A)N6–H6· · ·N3(G) and (G)N2–H2· · ·N7(A) hydrogen bonds correlated by the $^{2h}J_{N6N3}$ and $^{2h}J_{N2N7}$ coupling constants, respectively. (b, c) Magnetization transfer pathways used in the H2N6N3 (b) and (H6)N6N3H2 pulse sequences for correlating the (A)H2 proton (ω_2) with the (G)N3 nitrogen (ω_1).

tal piece of information, namely, evidence for the (A5)N6H6· · ·N3(G3) hydrogen bond, eluded us, since the A5 amino ($N6H6_{1,2}$) protons were severely exchange broadened. An examination of the ^1H–^{15}N HSQC spectrum (0 °C) at very low contour levels revealed broad $H6_{1,2}$–N6 cross peaks separated by ∼0.5 ppm, suggesting the possibility of weak hydrogen bonding and, consequently, a small $^{2h}J_{N6N3}$ coupling constant. The combination of exchange broadening and small $^{2h}J_{N6N3}$ resulted in no observable (A5)N6H6–N3(G3) cross peaks in the HNN–COSY spectrum and it became neccessary to use non-exchangeable protons to probe this critical hydrogen bond. The nearest non-exchangeable proton appropriate for this purpose happens to be H2 of adenine (Figure 1a), which is separated from the N6 nitrogen by *four bonds*. This neccessitated the development of a different route to detect the $^{2h}J_{NN}$ coupling on such a remote proton.

In this work, we present pulse-sequences to establish the presence of the (A5)N6H6 · · · N3(G3) hydrogen bond using the H2 proton as a reporter. Two different magnetization transfer strategies are presented: an out and back method (the H2N6N3 experiment) which is well-suited for samples in D_2O solution, and a straight-through (the (H6)N6N3H2 experiment) approach which is appropriate for samples in H_2O solution. In the process, we extend the scope of non-exchangeable proton detected $^{2h}J_{NN}$ correlated spectroscopy to include reporter protons which are removed from the hydrogen bond site by two magnetization transfer steps (see below). The methods are first demonstrated on the system $d(G_1G_2G_3T_4T_5C_6A_7G_8G_9)_2$ (Figure 2c) whose solution structure has recently been determined by NMR (Kettani et al., 2000b), and contains a G3·(C6–A7) triad element (Figure 2d) in which G3 and A7 form a sheared G·A mismatch. This is a good test system, since all exchangeable proton resonances within the triad are observable, and therefore, the $^{2h}J_{N7N2}$ and $^{2h}J_{N6N3}$ are readily detectable by a combination of HNN-COSY and soft HNN-COSY techniques, which serve to validate the results of the H2N6N3 and (H6)N6N3H2 experiments. The techniques are then extended to the $d(GGGCAGGT)_4$ system in order

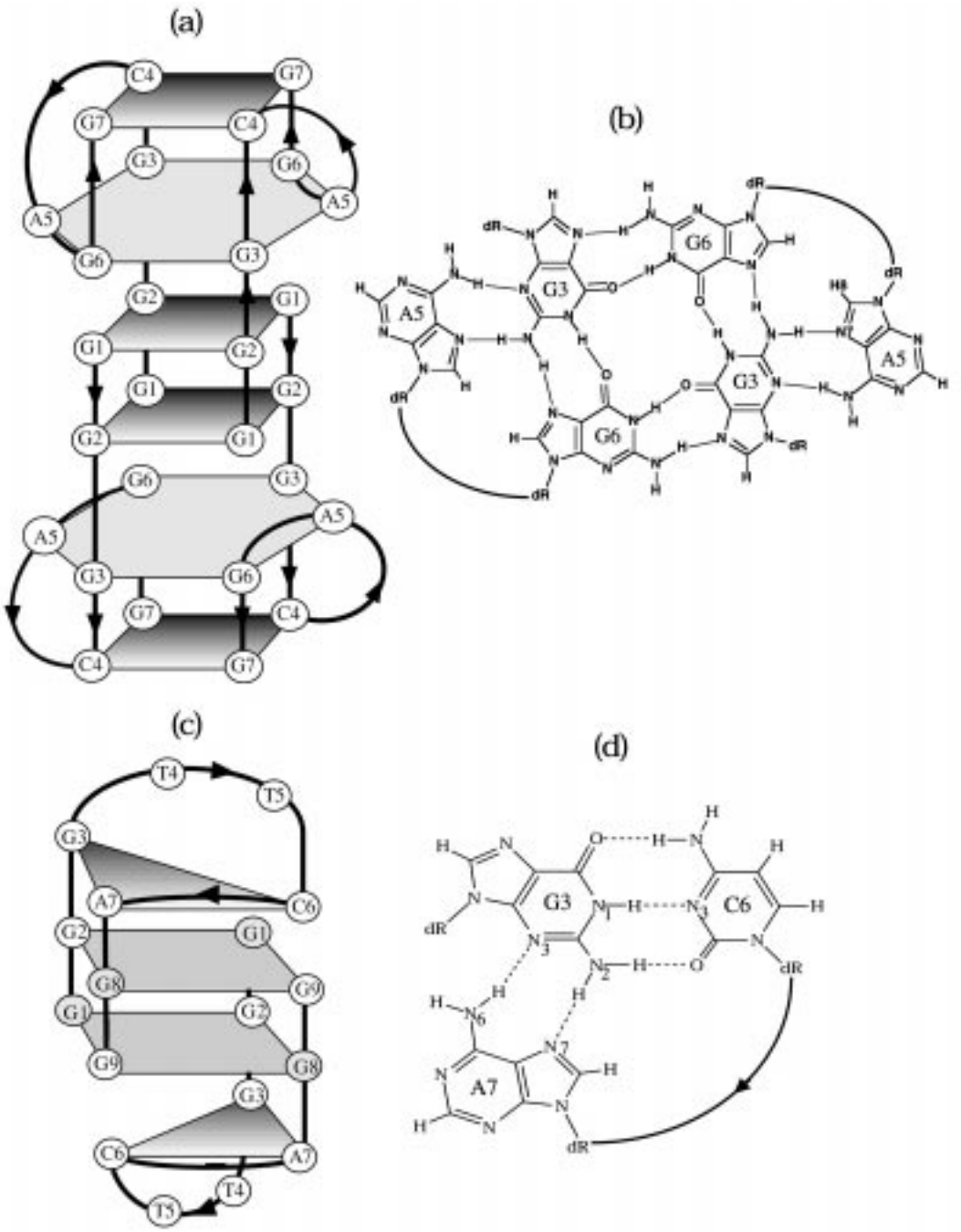

Figure 2. Schematic representations of the systems studied in this work: the d($G_1G_2G_3C_4A_5G_6G_7T_8$)$_4$ molecule (a) (excluding the terminal T8), in which the A5·(G3·G6·G3·G6)·A5 hexad motif (b) contains a sheared G3·A5 mismatch, and the d($G_1G_2G_3T_4T_5C_6A_7G_8G_9$)$_2$ molecule (c) in which the G3·(C6·A7) triad motif contains a sheared G3·A7 mismatch (d).

to establish the presence of the A·(GGGG)·A hexad motif.

NMR spectroscopy

The objective in the detection of the (A5)N6H6···N3 (G3) hydrogen bond via the H2 proton of adenine is to correlate H2 (ω_2) with the N3 nitrogen of guanine (ω_1). Although H2 is separated from N6 via four intervening bonds, the *coupling pathway* is much shorter, since H2 is directly coupled to C6 via a 10–11 Hz $^3J_{CH}$ long-range coupling (all coupling constant information has been obtained from Wijmenga and van Buuren (1998)). Furthermore, the $^1J_{C6N6}$ coupling is also fairly large (20–22 Hz). Therefore, two magnetization transfer steps (via $^3J_{H2C6}$ and $^1J_{C6N6}$) are sufficient to correlate H2 with N6, which can then communicate with N3 through the $^{2h}J_{N6N3}$ coupling. The two complementary approaches to achieve the desired objective (the H2N6N3 and (H6)N6N3H2) experiments) are described below in detail.

The out-and-back (H2N6N3) method

In this straightforward scheme (Figure 1b), magnetization originates and terminates on the H2 proton. The pulse sequence is shown in Figure 3a. The magnetization transfer pathway (ignoring trigonometeric coefficients) until the beginning of the t_1 period is outlined briefly below:

$$
\begin{aligned}
H_{2y} &\xrightarrow{^3J_{H2C6}} H_{2x}C_{6z} \xrightarrow{90^H_y,90^C_x} H_{2z}C_{6y} \\
&\xrightarrow{^1J_{C6N6}} H_{2z}C_{6x}N_{6z} \\
&\xrightarrow{90^C_y,90^N_x} H_{2z}C_{6z}N_{6y} \\
&\xrightarrow{^{2h}J_{NN}} (H_{2z}C_{6z}N_{6y} + H_{2z}C_{6z}N_{6x}N_{3z}) \\
&\xrightarrow{90^N_y} (H_{2z}C_{6z}N_{6y} + H_{2z}C_{6z}N_{6z}N_{3x})\ (t_1)
\end{aligned}
$$

A symmetrical sequence of steps returns the magnetization to the H2 proton for detection (t_2). The final spectrum consists of auto peaks centered at H2(ω_2),N6(ω_1) and cross peaks centered at H2(ω_2),N3(ω_1). Details pertaining to the use of selective pulses and tuning of delays, are described in the legend to Figure 3a. The most critical issue in this sequence is the N6 → N3 transfer period whose total duration is $4 \times T_{nn}$ (Figure 3a). Since the N6 magnetization is anti phase with respect to the H2 proton throughout this period, it is not feasible to carry out ^{1}H decoupling. This proves to be costly, especially if T_{nn} is necessarily long due to a small value for $^{2h}J_{NN}$ (in this study: $4 \times T_{nn} \sim 100$ ms), because of extensive dipolar relaxation of the N6 nitrogen with its two attached protons. In fact, it was impossible to perform this experiment in H_2O solution, especially at temperatures below 20 °C because of unfavorable relaxation. Above 20 °C, the hydrogen bond weakened even further, thereby reducing the $^{2h}J_{NN}$ coupling and lowering the sensitivity beyond detectable limits. One possible solution to the problem was to generate in phase C6 magnetization via H2–C6 heteronuclear cross-polarization (Majumdar et al., 1993; Zuiderweg, 1990). However, simulations showed that in the presence of a large, competing $^1J_{H2C2}$ coupling, hetero-CP transfer via the much smaller $^3J_{H2C6}$ is highly inefficient (< 1%). Due to the rather small chemical shift difference between C2 and C6 (∼2–3 ppm), it was not possible to achieve exclusive H2–C6 cross polarization without interference from the $^1J_{H2C2}$ coupling pathway. The easier solution lay in performing the experiment in D_2O, where the exchangeable amino protons are replaced by ^{2}H. Proton decoupling may be replaced with deuterium decoupling (Grzesiek et al., 1993) during the T_{nn} period, resulting in significantly reduced dipolar relaxation of the N6 coherence. An issue in this context is whether isotopic substitution has any deleterious effect on the $^{2h}J_{NN}$ coupling constant itself, which might further compromise the sensitivity of the experiment. Measurement of $^{2h}J_{NN}$ couplings in the $d(GGGTTCAGG)_2$ system, indicates (data not shown) that the $^{2h}J_{NN}$ values are identical within 0.2–0.3 Hz, upon going from H_2O to D_2O solution.

The relaxation of the $N_{6x,y}H_{2z}$ coherence will also be affected by the T_1 of the H2 proton, especially if T_{nn} is long. Fortunately, the H2 proton is a reasonably slow relaxing nucleus because of the relatively low proton density in its vicinity.

The straight-through ((H6)N6N3H2) method

The magnetization transfer pathway, shown schematically in Figure 1b, originates on the amino ($H6_{1,2}$) protons and terminates on the H2 proton. The pulse-sequence is shown in Figure 3b and a product operator

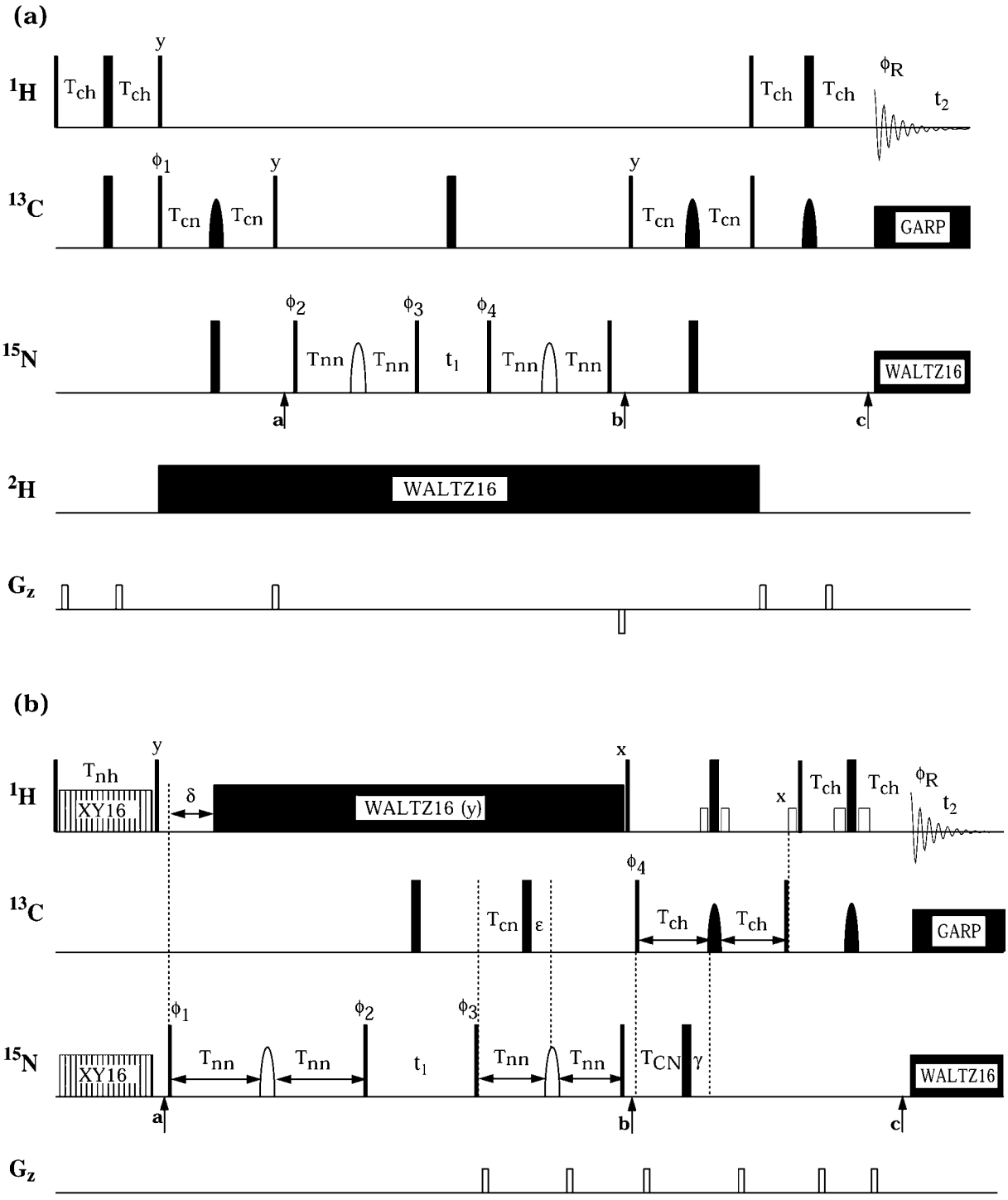
(a)
1H
Tch
Tch
y
Tch
Tch
ϕR
t2
13C
ϕ1
y
y
Tcn
Tcn
Tcn
Tcn
GARP
15N
ϕ2
ϕ3
ϕ4
Tnn
Tnn
t1
Tnn
Tnn
WALTZ16
a
b
c
2H
WALTZ16
Gz
(b)
1H
Tnh
XY16
y
δ
WALTZ16 (y)
x
x
Tch
Tch
ϕR
t2
13C
ϕ4
Tcn
ε
Tch
Tch
GARP
15N
ϕ1
ϕ2
ϕ3
XY16
Tnn
Tnn
t1
Tnn
Tnn
TCN
γ
WALTZ16
a
b
c
Gz

Figure 3. Pulse sequences for the H2N6N3 (a) and (H6)N6N3H2 (b) experiments. Narrow and thick solid lines represent high power 90° and 180° pulses, respectively, applied with phase x wherever unspecified. Open rectangles indicate low power square pulses. Solid and open sine-bell lobes indicate shaped pulses. High power pulses were applied with rf field strengths of 45 kHz (^{1}H), 18.5 kHz (^{13}C) and 6.6 kHz (^{15}N). The ^{1}H carrier was placed at 4.8 ppm in all experiments. (a) The ^{13}C carrier was centered at 159 ppm. During the $2 \times T_{ch}$ period, a 2 ms G3 pulse (Emsley and Bodenhausen, 1990) was used to prevent excitation of the C4 resonances ($\delta_{C4} \sim 151$–154 ppm) in order to refocus the $^3J_{H2C4}$ coupling ($\sim$11 Hz). The delay T_{ch} was adjusted to refocus the $^1J_{H2C2}$ ($\sim$200 Hz) coupling. During the $2 \times T_{cn}$ period, the same 2 ms G3 pulse was used to avoid excitation of the C5 resonance ($\delta_{C5} \sim 120$ ppm) to refocus the $^1J_{C6C5}$ coupling ($\sim$75 Hz in adenine). The ^{15}N carrier was centered at 82 ppm (N6) until point **a** (indicated with an arrow) where it was switched to 120 ppm, and back to 82 ppm at point **b** (arrow), and finally to 220 ppm at point **c** (arrow). During the $2 \times T_{nn}$ period, the intraresidue $^2J_{N6N1}$ coupling ($\sim$5 Hz) is active. This needs to be avoided, especially if $^{2h}J_{NN} < {}^2J_{N6N1}$ (as in the case under study). N1 excitation was avoided by employing a cosine-modulated G3 pulse with two excitation points, at the N6 (80 ppm) and N3 (160 ppm) frequencies. The pulse duration (2.8 ms) was carefully adjusted to avoid phase distortions of the N6 coherence (Sklenár et al., 1999) (the Varian software *pulsetool* was used for simulation purposes). The ^{2}H carrier was centered at 4 ppm and WALTZ16 (Shaka et al., 1983) decoupling was carried out using an rf field strength of 1 kHz. Delays used were: $T_{ch} = 14.5$ ms, $T_{cn} = 9$ ms, $T_{nn} = 25$ ms. 4 kHz GARP (Shaka et al., 1985) ^{13}C and 1 kHz WALTZ16 ^{15}N decoupling were employed during acquisition. Phase cycles: $\phi_1 = x, -x, \phi_2 = x, x, -x, -x, \phi_3 = 4(y), 4(-y), \phi_4 = 8(y), 8(-y), \phi_R = x, -x, -x, x$. Quadrature-detection along ω_1 was achieved via States-TPPI (Marion et al., 1989) phase cycling of ϕ_2 and ϕ_3. All gradients were applied as rectangular z-gradients, of duration 0.5 ms and strength $\sim$15 G/cm. (b) rf field strengths used for the XY-16 sequence were 45 (^{1}H) and 4.5 kHz (^{15}N). The ^{1}H WALTZ16 decoupling field strength was 6.25 kHz. Water-flipback (Grzesiek and Bax, 1993) and WATERGATE (Piotto et al., 1992) was achieved using 1.9 ms square pulses. ^{15}N carrier shifts, ^{13}C,^{15}N shaped pulses and the delays T_{ch}, T_{cn} and T_{nn} were identical to those in Figure 2a. $T_{nh} = 5.5$ ms, $\delta = 2.75$ ms ($1/4J_{NH}$), $\epsilon = T_{nn} - T_{cn}$ and $\gamma = T_{ch} - T_{cn}$. Phase cycling: $\phi_1 = x, -x, \phi_2 = x, x, -x, -x, \phi_3 = 4(x), 4(-x), \phi_4 = 8(x), 8(-x), \phi_R = 4(x, -x), 4(-x, x)$. Quadrature-detection along ω_1 was achieved via States-TPPI phase cycling of ϕ_1 and ϕ_2. For the H8N9N3 experiment, the H2N6N3 sequence was modified as follows: ^{13}C carrier: 140 ppm; ^{15}N carrier: 165 ppm between **a** and **b**, 170 ppm otherwise. The shaped ^{13}C pulse in the center of the T_{CH} period was replaced by a hard, 18.5 kHz pulse, and the hard ^{15}N pulse in the center of the T_{cn} period was replaced by a 2.0 ms G3 pulse. Delays were: $T_{ch} = 1.3$ ms, $T_{cn} = 10$ ms, $T_{nn} = 25$ ms. During acquisition (t_2), no ^{15}N decoupling, and 3.3 kHz ^{13}C, GARP decoupling was employed.

outline is as follows:

$$
\begin{aligned}
N_{6y}(H_{6,1z} + H_{6,2z}) &\xrightarrow{^1J_{N6H6}} N_{6x}\,, \xrightarrow{^{2h}J_{NN}} (N_{6x} + N_{6y}N_{3z}) \\
&\xrightarrow{90^N_x} (N_{6x} + N_{6z}N_{3y})\ (t_1) \xrightarrow{90^N_x} \\
(N_{6x} + N_{6y}N_{3z}) &\xrightarrow{^{2h}J_{NN}} \xrightarrow{^1J_{C6N6}} N_{6y}C_{6z} \\
&\xrightarrow{90^C_x,90^N_x} N_{6z}C_{6y} \\
&\xrightarrow{^1J_{C6N6}} \xrightarrow{^3J_{C6H2}} C_{6y}H_{2z} \\
&\xrightarrow{90^H_x,90^C_x} C_{6z}H_{2y} \xrightarrow{^3J_{H2C6}} H_{2x}\,(t_2)
\end{aligned}
$$

To achieve efficient transfer between exchange broadened NH_2 protons and the N6 nitrogen, an XY-16 CPMG sequence (Gullion et al., 1990; Mueller et al., 1995; Mulder et al., 1996) was employed. The quenching of exchange broadening rates under spin-locked conditions depends on a variety of factors such as exchange lifetimes, chemical shift differences of the exchanging protons, strength of the spin-locking field, pulse repetition rates and relaxation effects (Krishnan and Rance, 1995). For the system under study, we examined the competing effects of relaxation and rotational exchange as a function of temperature. The 1D spectra in Figures 4a–d, show the temperature dependence of INEPT and CPMG-based intra-residue $H6_{1,2} \rightarrow N6 \rightarrow C6 \rightarrow H2$ transfer efficiencies, at 600 MHz (^{1}H). It is clear that in the temperature range 10–30 °C, intermediate exchange-broadening and favorable relaxation conditions prevail and therefore, spin-locking has a dramatic effect on signal intensity, with almost an order of magnitude enhancement at 20 °C. At lower temperatures, under slow exchange conditions, unfavorable relaxation effects dominate, to significantly attenuate the spin-locking enhancement. At higher temperatures, in the fast exchange and favorable relaxation regime, the INEPT and CPMG intensities tend to become comparable. However, weak hydrogen bonds may not be stable enough at higher temperatures. Therefore, the optimal temperature is the one where the CPMG based transfer is most efficient without compromising the hydrogen bond stability. In our study, we chose 20 °C to carry out these experiments on the basis of the results in Figure 4 and melting properties of the sample.

As discussed above, N6-H dipolar relaxation during the long T_{nn} period is active and may degrade the sensitivity. However, since the N6 coherence is in-phase with respect to proton, ^{1}H decoupling is feasible in this experiment and consequently, N6 relaxation is less severe. In addition, since a number of transfer steps may be concatenated in this sequence, it is significantly shorter (typically 120–140 ms) relative to its out-and-back counterpart (typically 180–200 ms), which further ameliorates relaxation effects. Other issues pertaining to the timing of delays and selective pulses are identical to the H2N6N3 experiment.

Assignment of N3 resonances

An important issue in this experiment is the assignment of the guanine N3 resonances. This was achieved via an H8(ω_2) $\rightarrow$ (N9,N3)(ω_1) COSY experiment (H8N9N3), a precursor to which has been described previously (Kettani et al., 2000b). The sequence is a simple modification of the H2N6N3 sequence. Experimental details are provided in the legend to Figure 3, and a brief product operator description (until the beginning of the t_1 period) is given below:

$$\begin{aligned} H_{8y} &\xrightarrow{^1J_{H8C8}} \xrightarrow{90^H_y,90^C_x} H_{8z}C_{8y} \xrightarrow{^1J_{C8N9}} H_{8z}C_{8x}N_{9z} \\ &\xrightarrow{90^C_y,90^N_x} H_{8z}C_{8z}N_{9y} \\ &\xrightarrow{^2J_{N9N3}} (H_{8z}C_{8z}N_{9y} + H_{8z}C_{8z}N_{9x}N_{3z}) \\ &\xrightarrow{90^N_y} (H_{8z}C_{8z}N_{9y} + H_{8z}C_{8z}N_{9z}N_{3x})(t_1) \end{aligned}$$

A symmetrical sequence of steps returns magnetization to the H8 proton for detection. The spectrum consists of H8(ω_2),N9(ω_1) (auto) and H8(ω_2),N3(ω_1) (cross) peaks of opposite signs. Once H8 protons are assigned independently, the N3 resonances may be identified from the H8N9N3 COSY spectrum.

Experimental methods

All experiments were recorded on uniformly ^{13}C,^{15}N labeled samples of d($G_1G_2G_3T_4T_5C_6A_7G_8$ G_9)$_2$ (Figure 5) and d($G_1G_2G_3C_4A_5G_6G_7T_8$)$_4$ (Figure 6), in 99% D_2O solution for the H2N6N3 experiment, and in 95% H_2O/5% D_2O solution for the (H6)N6N3H2 experiment, at a temperature of 20 °C. For the d($G_1G_2G_3T_4T_5C_6A_7G_8G_9$)$_2$ system, sample concentrations were 1.5 and 3 mM (oligomer concentration) for the H2N6N3 and (H6)N6N3H2 spectra, respectively. For the d($G_1G_2G_3C_4A_5G_6G_7T_8$)$_4$ sample, a 3 mM sample was used for both spectra. All data were recorded on Varian Inova spectrometers operating at 600 MHz (^{1}H), equipped with four rf channels, and actively shielded triple-resonance z-gradient probes. Data were processed using Felix 97.0 (Molecular Simulations, Inc.) software.

Results and discussion

The H2N6N3 and (H6)N6N3H2 sequences were test-driven on the DNA sample d($G_1G_2G_3T_4T_5$ $C_6A_7G_8G_9$)$_2$, consisting of a G1·G2·G8·G9 tetrad and a G3·(C6–A7) triad, whose solution structure has recently been solved by NMR in our laboratory (Kettani et al., 2000b; Al-Hashimi et al., in press). Within the triad element, the G3 and A7 residues pair via a sheared G·A alignment (Figure 2d). All exchangeable protons in the triad are sharp and well-defined, and therefore, all N–H···N hydrogen bond connectivities are readily identified using combinations of HNN–COSY and soft HNN–COSY experiments (data not shown). Figures 5a and 5b show regions of H2N6N3 and (H6)N6N3H2 spectra, respectively, of this system. Both spectra are identical in content, consisting of (A7)H2–N6(A7) (auto) and (A7)H2–N3(G3) (cross) peaks (of opposite signs), and thereby report on the (A7)N6H6···N3(G3) hydrogen bond via the non-

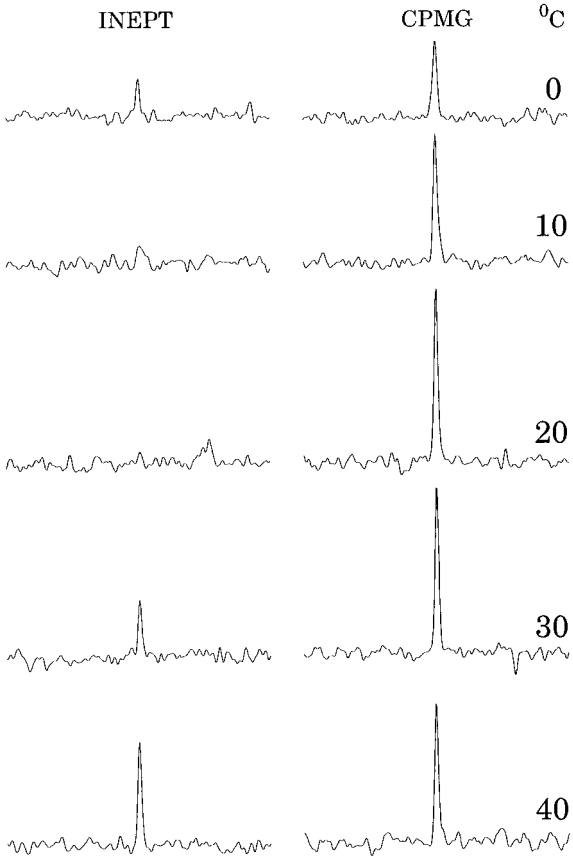

Figure 4. Comparison of INEPT and XY-16 based CPMG sequences for $H6_{1,2}$ $\rightarrow$ N6 transfer as a function of temperature, in the A5 residue of the d($G_1G_2G_3C_4A_5G_6G_7T_8$)$_4$ sample. One-dimensional spectra were recorded at 14.1 T (600 MHz, ^{1}H frequency), using a modification of the sequence shown in Figure 3b, adopting a $H6_{1,2}$ $\rightarrow$ N6 $\rightarrow$ C6 $\rightarrow$ H2 pathway. The delay time T_{nh} was optimized for maximum intensity (in the range 5–5.5 ms), wherever possible.

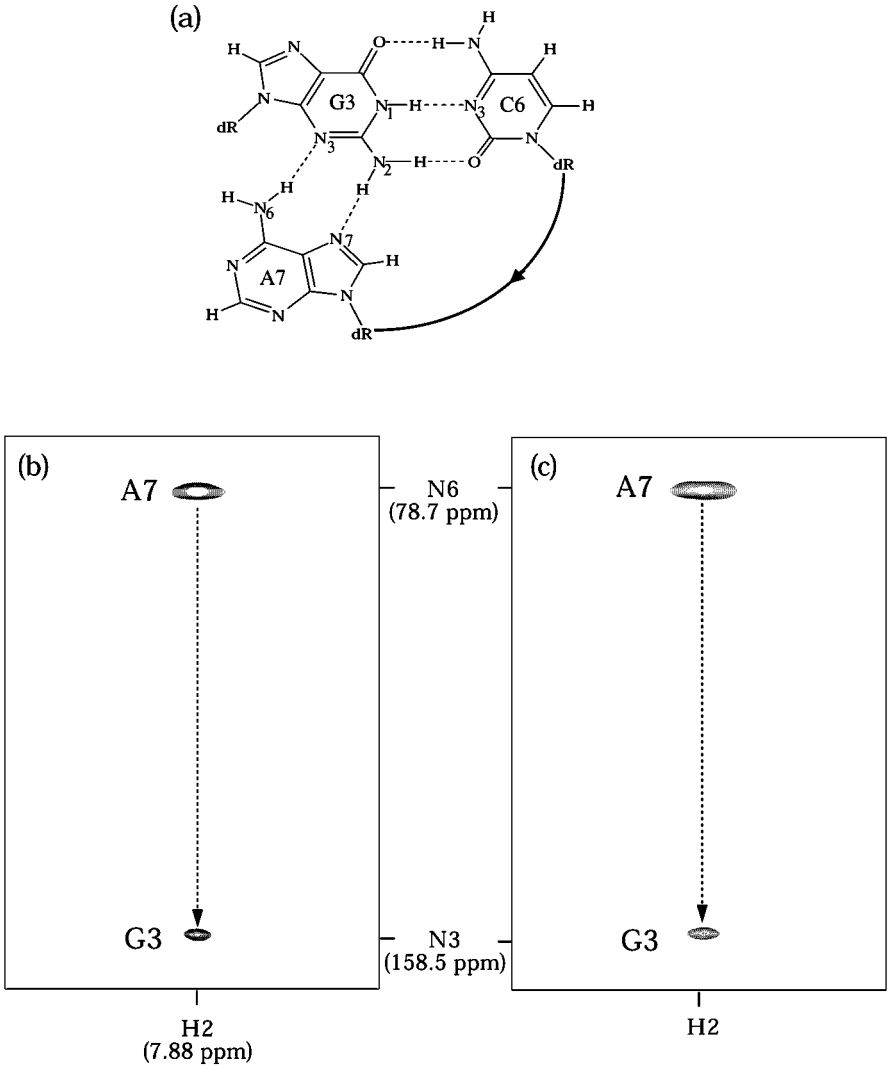

Figure 5. (a) H2N6N3 and (b) (N6)H6N3H2 spectra (20 °C, 600 MHz, ^{1}H frequency) showing (A7)H2–N6(A7) (auto) and (A7)H2–N3(G3) (cross) peaks establishing the (A7)N6H6$_{1,2}$ · · ·N3(G3) hydrogen bond in the sheared G3·A7 mismatch within the G3·(C6-A7) triad motif of the d(G$_1$G$_2$G$_3$T$_4$T$_5$C$_6$A$_7$G$_8$G$_9$)$_2$ molecule (Figures 2c,d). For both spectra, 64 transients were acquired with 544 (t_2) × 50 (t_1) complex points, spectral widths of 8000 (ω_2) × 7000 (ω_1) Hz, relaxation delays of 1.6 (a) and 1.5 (b) seconds and total data collection time of about 3 h.

exchangeable H2 proton of A7. N3 assignments were obtained from a previously described variation of the H8N9N3 COSY experiment (Kettani et al., 2000b). The $^{2h}J_{N6N3}$ coupling measured from the H2N6N3 and (H6)N6N3H2 spectra (3.2 Hz) was in close agreement with that obtained from the HNN-COSY spectrum (3.4 Hz).

Figures 6a and 6b show regions of H2N6N3 and (H6)N6N3H2 spectra respectively, recorded on the larger d(G$_1$G$_2$G$_3$C$_4$A$_5$G$_6$G$_7$T$_8$)$_4$ system, consisting of (H2–N6) (auto) and (H2,N3) (cross) peaks, thereby unambiguously establishing the existence of an (A5)N6H6 · · ·N3(G) hydrogen bond. The H2,N3 cross-peak is easily assigned to G3 from the H8N9N3 COSY spectrum in Figure 6c, showing (H8–N9) auto- and (H8–N3) cross-peaks belonging to the five guanine residues in the molecule. The H8 proton assignments were made independently, based on NOE and H(CC)NH TOCSY (Fiala et al., 1996) data. With this observation, the validation of the sheared G3·A5 base pair and consequently, the A5·(G3·G6·G3·G6)·A5 hexad, is complete.

A calculation of the $^{2h}J_{N6N3}$ coupling constant based on the ratio of the cross and diagonal peak

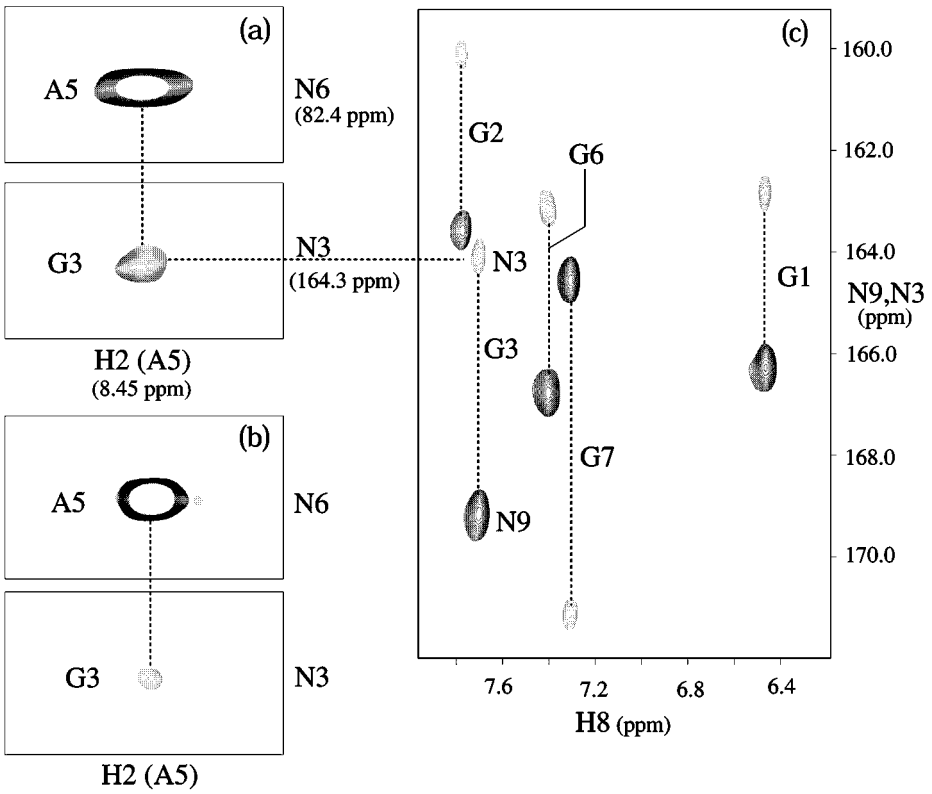

Figure 6. (a) H2N6N3 and (b) (N6)H6N3H2 spectra showing (A5)H2–N6(A5) (auto) and (A5)H2–N3(G3) (cross) peaks establishing the presence of the (A5)N6H6$_{1,2}$ ···N3(G3) hydrogen bond in the sheared G3·A5 mismatch within the hexad motif of the d($G_1G_2G_3C_4A_5G_6G_7T_8$)$_4$ system (Figures 2a,b). The H8N9N3 spectrum (c) shows H8–N9 (auto, solid contours) and H8–N3 (cross, grey contours) peaks belonging to the five guanine residues in the sample, used for assigning the H2–N3 cross peak in (a) and (b) to the G3 residue. All spectra were recorded at 20 °C on a Varian INOVA spectrometer operating at 600 MHz (^{1}H). Data acquisition details: (a). transients: 160, complex points: 544 (t_2) × 75 (t_1), spectral widths: 8000 (ω_2) × 6000 (ω_1) Hz, relaxation delay: 1.6 s, total data collection time: 13 h. (b) transients: 160, complex points: 512 (t_2) × 75 (t_1), spectral widths: 7000 (ω_2) × 6075 (ω_1) Hz, relaxation delay: 1.5 s, total data collection time: 13 h. (c) transients: 160, complex points: 544 (t_2) × 60 (t_1), spectral widths: 8000 (ω_2) × 1720 Hz, total data collection time: 12 h.

(Vuister and Bax, 1993; Dingley and Grzesiek, 1998) yielded a value of 1.7 ±0.5 Hz. This low value is in keeping with the weakness of the hydrogen bond indicated by HSQC spectra (see Introduction).

As mentioned above, the relative sensitivity of the two experimental approaches depends on a number of factors, and therefore, direct comparison is often difficult. The H2N6N3 sequence is longer, but N6–^{2}H relaxation is more favorable in D_2O. The (H6)N6N3H2 method is shorter by almost 40%, but is affected by N6–H6$_{1,2}$ dipolar relaxation during the 4 × T_{nn} period, and depends rather critically on the extent to which exchange-broadening of the H6$_{1,2}$ resonances is quenched by spin-locking. In the d(GGGCAGGT)$_4$ system, the H2N6N3 sequence clearly performs better than the (H6)N6N3H2 experiment at 600 MHz. Whether this is an outcome of the competitive factors discussed above or due to technical reasons such as a long-term degradation in spectrometer performance under spin-locking conditions, is not clear at the moment.

In summary, we have presented two experimental approaches to identify (A)N6H6 ··· N3(G) sheared G·A mismatches using the non-exchangeable H2 proton of adenine as a reporter. These techniques serve as useful alternatives under conditions of severe exchange broadening of hydrogen bonded amino protons. For small $^{2h}J_{N6N3}$ coupling constants, such as in the present study, these experiments are likely to be successful for intermediate-sized molecules in the 10–15 kD range. For larger $^{2h}J_{N6N3}$ couplings, they are likely to be applicable to even larger systems. Development of methods for addressing more challenging systems is currently in progress.

Acknowledgements

This research was supported under grant no. GM34504 to DJP. We thank Dr Burkhard Luy for useful discussions and suggestions.

References

Al-Hashimi, H., Majumdar, A., Gorin, A., Kettani, A., Skripkin, E. and Patel, D.J. (2001) *J. Am. Chem. Soc.*, in press.

Cai, Z., Gorin, R., Frederick, R., Ye, X., Hu, W., Majumdar, A., Kettani, A. and Patel, D.J. (1998) *Nat. Struct. Biol.*, **5**, 203–212.

Cate, J.H., Gooding, A.R., Podell, E., Zhou, K., Golden, B.L., Kundrot, C.E., Cech, T.E. and Doudna, J.A. (1996) *Science*, **273**, 1678–1685.

Chou, S.H., Cheng, J.W. and Reid, B.R. (1992) *J. Mol. Biol.*, **228**, 138–155.

Chou, S.H., Zhu., L. and Reid, B.R. (1997) *J. Mol. Biol.*, **267**, 1055–1067.

Dingley, A.J. and Grzesiek, S. (1998) *J. Am. Chem. Soc.*, **120**, 8293–8297.

Dingley, A.J., Masse, J.E., Feigon, J. and Grzesiek, S. (2000) *J. Biomol. NMR*, **16**, 279–289.

Dingley, A.J., Masse, J.E., Peterson, R.D., Barfield, M., Feigon, J. and Grzesiek, S. (1999) *J. Am. Chem. Soc.*, **121**, 6019–6027.

Emsley, L. and Bodenhausen, G. (1990) *Chem. Phys. Lett.*, **165**, 469.

Farmer II, B.T. and Venters, R.A. (1998) In *Biological Magnetic Resonance Vol. 16* (Ed., Rama Krishna, N. and Berliner, L.J.), Kluwer Academic Publishers/Plenum, New York, NY, pp. 75–120.

Fiala, R., Jiang, F. and Patel, D.J. (1996) *J. Am. Chem. Soc.*, **118**, 689–690.

Gardner, K.H. and Kay, L.E. (1998) In *Biological Magnetic Resonance Vol. 16* (Ed., Rama Krishna, N. and Berliner, L. J.), Kluwer Academic Publishers/Plenum, New York, NY, pp. 27–74.

Gautheret, D., Konnings, D. and Gutell, R.R. (1994) *J. Mol. Biol.*, **242**, 1–8.

Gemmecker, G. (2000) *Angew. Chem. Int. Ed. Engl.*, **39**, 1224–1226.

Grzesiek, S., Anglister, J., Ren H. and Bax, A. (1993) *J. Am. Chem. Soc.*, **115**, 4369–4370.

Grzesiek, S. and Bax, A. (1993) *J. Am. Chem. Soc.*, **115**, 12593–12594.

Gullion, T., Baker, D.B. and Conradi, M.S. (1990) *J. Magn. Reson.*, **89**, 479.

Hennig, M. and Geierstanger, B.H. (1999) *J. Am. Chem. Soc.*, **121**, 5123–5126.

Hennig, M. and Williamson, J.R. (2000) *Nucleic Acids Res.*, **28**, 1585–1593.

Heus, H.A. and Pardi, A. (1991) *Science*, **253**, 191–194.

Hirao I., Kawai G., Yoshizawa S., Nishimura Y., Ishido Y., Watanabe K. and Miura K. (1994) *Nucleic Acids Res.*, **22**, 576–582.

Hirao, I., Nishimura, Y., Naraoka, T., Watanabe, K., Arata, Y. and Miura, K. (1989) *Nucleic Acids Res.*, **17**, 2223–2231.

Jiang, F., Gorin, A., Hu, W., Majumdar, A., Baskerville, S., Xu W., Ellington, A. and Patel, D.J. (1999a) *Structure*, **7**, 1461–1472.

Jiang, L., Majumdar, A., Hu, W., Jaishree, T.J., Xu, W. and Patel, D. J. (1999b) *Structure*, **7**, 817–827.

Jucker, F.M., Heus, H.A., Yip, P.F., Moors, E.H. and Pardi, A.A. (1996) *J. Mol. Biol.*, **264**, 968–980.

Kettani, A., Bouaziz, S., Skripkin, E., Majumdar, A., Wang, W., Jones, R.A. and Patel, D.J. (1999) *Structure*, **7**, 803–815.

Kettani, A., Gorin, A., Majumdar, A., Hermann, T., Skripkin, E., Zhao, H. and Jones R. (2000a) *J. Mol. Biol.*, **297**, 627–644.

Kettani, A., Basu, G., Gorin, A., Majumdar, A., Skripkin, E. and Patel, D. J. (2000b) *J. Mol. Biol.*, **301**, 129–146.

Krishnan, V.V. and Rance, M. (1995) *J. Magn. Reson.*, **A116**, 97–106.

Legault, P., Li, J., Mogridge, J., Kay, L.E. and Greenblatt, J. (1998) *Cell*, **93**, 289–299.

Li, Y., Zon and Wilson, W.D. (1991) *Proc. Natl. Acad. Sci. USA*, **88**, 26–30.

Lin, C.H. and Patel, D.J. (1997) *Chem. Biol.*, **4**, 817–832.

Lin, C.H., Wang, W., Jones, R.A. and Patel, D.J. (1998) *Chem. Biol.*, **5**, 555–572.

Liu, A., Majumdar, A., Hu, W., Kettani, A., Skripkin E. and Patel, D. J. (2000) *J. Am. Chem. Soc.*, **122**, 3206–3210.

Luy, B. and Marino, J. (2000) *J. Am. Chem. Soc.*, **122**, 8095–8096.

Majumdar, A., Wang, H., Morshauser, R.C. and Zuiderweg, E.R.P. (1993) *J. Biomol. NMR*, **3**, 387–397.

Majumdar, A., Kettani, A. and Skripkin, E. (1999a) *J. Biomol. NMR*, **14**, 67–70.

Majumdar, A., Kettani, A. and Skripkin, E. and Patel, D. J. (1999) *J. Biomol. NMR*, **15**, 207–211.

Marion, D., Ikura, M., Tschudin, R. and Bax, A. (1989) *J. Magn. Reson.*, **85**, 393–399.

Maskos, M., Gunn, B.M., LeBlanc, D.A., Morden, K.M. (1993) *Biochemistry*, **32**, 3583–3595.

Mollova, E.T. and Pardi (2000) *Curr. Opin. Struct. Biol.*, **10**, 298–302.

Mueller, L., Legault, P. and Pardi, A. (1995) *J. Am. Chem. Soc.*, **117**, 11043–11048.

Mulder, F.A.A, Spronk, C.A.E.M., Slijper, M., Kaptein, R., Boelens, R. (1996) *J. Biomol. NMR*, **8**, 223–228.

Pervushin, K., Ono, A., Fernandez, A., Szyperski, T., Kainosho, M. and Wüthrich, K. (1998) *Proc. Natl. Acad. Sci. USA*, **95**, 14147–14151.

Piotto, M., Saudek, V. and Sklenár, V. (1992) *J. Biomol. NMR*, **2**, 661–665.

Pley, H.W., Flaherty, K.M., McKay, D.B. (1994) *Nature*, **372**, 68–74.

Shaka, A.J., Keeler, J. and Freeman, R. (1983) *J. Magn. Reson.*, **52**, 335–338.

Shaka, A.J. and Keeler, J. (1987) *Prog. NMR Spectrosc.*, **19**, 49–192.

Sklenár, V., Masse, J.E. and Feigon, J. (1999) *J. Magn. Reson.*, **137**, 345–349.

Szewczak, A.A., Moore, P.B., Chang, Y.L. and Wool, I.G. (1993) *Proc. Natl. Acad. Sci. USA*, **90**, 9581–9585.

Wijmenga, S.S. and van Buuren, B.N.M. (1998) *Prog. NMR Spectrosc.*, **32**, 287–387.

Wohnert, J., Dingley, A.J., Stoldt, M., Gorlach, M., Grzesiek S. and Brown, L.R. (1999) *Nucleic Acids Res.*, **27**, 3104–3110.

Vuister, G. and Bax, A. (1993) *J. Am. Chem. Soc.*, **115**, 7772–7777.

Zuiderweg, E.R.P. (1990) *J. Magn. Reson.*, **89**, 533–542.